Molecular Neurobiology (2025) 62:7805–7819
https://doi.org/10.1007/s12035-025-04736-5

RESEARCH

miR-758-3p Interferes with Neuronal Apoptosis in Cerebral Ischemia–Reperfusion by Inhibiting ILK

Xiaoli Min[1] · Xuesong Bai[2,3] · Qing Zhao[1] · Wenwu Yang[1] · Sixian Lin[1] · Lei Xian[1] · Rui Jing[1] · Xuhui Li[4] · Wenji Jia[4] · Wei Miao[4] · Mei Yin[4] · Feifei Shang[5] · Yong Zeng[6]

Received: 6 May 2024 / Accepted: 31 January 2025 / Published online: 12 February 2025

Abstract

This study investigated the role of integrin-linked kinase (ILK) in neuronal apoptosis induced by cerebral ischemia−reperfusion injury (CIRI) and its interaction with a circRNA (0000964) and miR-758-3p. Using in vivo and in vitro rat models, we clarified how ILK regulates neuronal apoptosis during CIRI. Our findings revealed that ILK expression is upregulated in response to CIRI and is modulated by the circRNA (0000964)/miR-758-3p axis. This study provides new insights into the molecular mechanisms of CIRI and suggests potential therapeutic targets to reduce neuronal apoptosis. A CIRI rat model was created through middle cerebral artery occlusion (MCAO). After miR-758-3p overexpression, neurological deficits, CIRI volume, and the expression levels of circRNAs (0000964) and ILK were evaluated. Neurons were subjected to oxygen−glucose deprivation (OGD) to simulate in vitro CIRI, and the same molecules were analyzed. MCAO-induced CIRI downregulated a circRNA (0000964) and upregulated ILK and miR-758-3p. Similarly, in vitro OGD-induced apoptosis downregulated a circRNA (0000964) and upregulated ILK and miR-758-3p. Further analysis confirmed that a circRNA (0000964) negatively regulates miR-758-3p, which in turn negatively regulates ILK. This axis controls ILK and Caspase-3 expression, influencing neuronal apoptosis. ILK has been identified as a key regulator of neuronal apoptosis in CIRI. The circRNA (0000964)/miR-758-3p axis modulates ILK, impacting neuronal survival. This molecular network offers new insights into CIRI pathophysiology and highlights possible therapeutic approaches.

Keywords ILK · CIRI · CircRNA (0000964) · MiR-758-3p · Neuronal apoptosis

Introduction

Ischemic cerebrovascular disease is a category of severe conditions that pose significant risks to life and health, with an increasing incidence rate that features high mortality and disability rates, imposing heavy economic burdens on societies and families [1]. The overall incidence rate in China was significantly higher than the global average for the same period, and China has become the leading cause of death among Chinese residents [2, 3]. The primary treatment for ischemic cerebrovascular disease involves revascularization to restore blood flow, improve hypoxic conditions, and

Xiaoli Min, Xuesong Bai, and Qing Zhao contributed equally

✉ Xiaoli Min
minxiaoli@kmmu.edu.cn

✉ Feifei Shang
Shang_feifei@126.com

✉ Yong Zeng
zengyong13888510388@163.com

[1] Department of Cerebrovascular Diseases, The Second Affiliated Hospital of Kunming Medical University, Kunming, China

[2] Department of Neurosurgery, Xuanwu Hospital, Capital Medical University, Beijing, China

[3] International Neuroscience Institute (China-INI), Beijing, China

[4] Department of Neurosurgery, The Second Affiliated Hospital of Kunming Medical University, Kunming, China

[5] Institute of Life Science, Chongqing Medical University, Chongqing, China

[6] Department of Psychiatry, The Second Affiliated Hospital of Kunming Medical University, Kunming, Yunnan, China

maintain a balance between energy supply and demand, thereby saving neurons that are close to death. However, reperfusion can trigger secondary brain damage, known as cerebral ischemia−reperfusion injury (CIRI) [4]. The pathomechanism of CIRI is highly complex and includes mitochondrial respiratory dysfunction, activation of calcium-sensitive proteases, intracellular calcium overload, excessive production of reactive oxygen species, lipid peroxidation damage, excitatory amino acid release, and inflammatory responses [5–7]. These factors interact and influence each other, ultimately resulting in secondary energy failure in neurons, promoting cell apoptosis, and worsening existing neurological deficits, especially in neuronal cells [8–11]. Recent studies have focused on the interactions between noncoding RNAs (such as circRNAs and miRNAs) and proteins. The complex network between these molecules plays a significant role in regulating neuronal apoptosis [12–15]. This study focused on exploring the effects of a circRNA (0000964) and miR-758-3p on ILK-mediated neuronal cell apoptosis after ischemic brain injury, with a particular emphasis on the role of integrin-linked kinase (ILK).

ILK is a critical protein kinase involved in a wide range of cellular processes, including adhesion, proliferation, migration, and survival [16]. Within the nervous system, the regulation of the expression and activity of ILK is vital for the function and survival of neurons. Previous studies have shown that ILK can be activated by the CXCL1/CXCR2 axis, mediating cell motility or migration and thereby stimulating neuronal growth [17, 18]. In certain neurological disorders, the regulation of the ILK/Akt pathway can intervene in Alzheimer's disease and age-related cognitive impairments [19–21]. These studies demonstrate that ILK may influence neuronal function by affecting the functionality of certain proteins. ILK participates in various intracellular signaling pathways by interacting with extracellular matrix components and intracellular signaling proteins [22–24], and the activation or inhibition of these pathways directly affects the survival and apoptosis of neurons. In the context of CIRI, the expression and function of ILK may be regulated by upstream noncoding RNAs. This study focused on the roles of a circRNA (0000964) and miR-758-3p in this process. As an emerging class of noncoding RNAs, circRNAs have attracted widespread attention because of their unique closed-loop structure and multifunctionality. By acting as sponges for miRNAs, circRNAs can regulate the function of miRNAs, thereby affecting the expression of downstream proteins [25, 26]. As a key miRNA, miR-758-3p plays roles in various physiological and pathological processes, including diseases of the nervous system [27, 28]. By exploring the regulatory mechanisms of circRNA (0000964) and miR-758-3p on ILK in depth, we aimed to reveal the role of this novel molecular network in neuronal apoptosis induced by CIRI, providing a new perspective for understanding the molecular mechanisms of CIRI and offering potential new targets for developing treatment strategies for these brain injuries.

Materials and Methods

Animal Husbandry

In this study, 48 male Sprague–Dawley (SD) rats, aged between 6 and 8 weeks, were utilized. The experiment was divided into two main batches: one batch of brain tissue was used for the TTC assay, while the other batch was used for all remaining experiments. These rats were procured from Beijing Vital River Laboratory Animal Technology Co., Ltd., and were maintained under an animal use license with the license number SCXK (Beijing) 2021–0011. Throughout the experiment, the rats were housed under specific conditions: a controlled environment with a constant temperature (22 ± 2 °C) and humidity ($55 \pm 10\%$) and a 12-h light−dark cycle. The rats were individually housed in standard cages to ensure ample space for activity, with access to clean drinking water and standard rodent chow. All animal experimental procedures were carried out in accordance with relevant ethical guidelines and protocols and were approved by the Animal Experiment Ethics Committee of Kunming Medical University, approval number: kmmu20220412.

Construction of a Middle Cerebral Artery Occlusion (MCAO) Model of Cerebral Infarction in Rats

The rats were grouped into the sham, CIRI, CIRI + miR-758-3p-NC, and CIRI + miR-758-3p groups, each containing 10 animals. The rats were anesthetized with 2% isoflurane (Cat# 792632, Sigma−Aldrich, Germany) and placed in a cranial borehole near the bregma. An electric electrode was used to inject miR-758-3p or control virus into the brain. The CIRI + miR-758-3p-NC group received 1.792 µL of control virus, whereas the CIRI + miR-758-3p group received 1.976 µL of the miR-758-3p virus. After 3 days, the right carotid artery complex was exposed and occluded. After 90 min, the ischemia was reversed, and the temperature was maintained at 37 °C. The brains of the rats ($n = 6$) were subsequently sectioned for fluorescence analysis to verify the efficiency of miR-758-3p infection. The brain sections were stained with DAPI, washed, and imaged under a fluorescence microscope, with green fluorescence indicating miR-758-3p transfection [29, 30].

Evaluation of Neurological Deficits via the Bederson Scoring Method

The commonly used Bederson scoring method categorizes the extent of impairment as follows: normal (grade 0): (1) no observable activity abnormalities, with both forelimbs

extending straight toward the ground when the rat is suspended by its tail. (2) When placed on a soft plastic board, gentle tail grasping and applying lateral thrust behind the shoulders of the rat to slide it approximately 10 cm yields equal resistance to pushing from both sides. Moderate (grade 1): (1) when the forelimb is suspended by its tail, the forelimb contralateral to the cerebral ischemia exhibits flexion, elevation, inward shoulder rotation, and elbow extension. (2) Essentially similar to grade 0. Severe (grade 2): (1) same as grade 1. (2) Similar to the previous method but with noticeably reduced lateral resistance on the side contralateral to the ischemic hemisphere [31, 32].

5-Triphenyltetrazolium Chloride (TTC) Staining

After the rats were euthanized ($n = 6$), their brain tissues were rapidly extracted and flash-frozen in a − 20 °C freezer for 20 min. The frozen brain tissues were then sectioned continuously along the coronal plane with a precooled sharp blade while still in a frozen state, with each section being 2 mm thick. The thick brain tissue sections were placed in a 2% solution of 2,3,5-triphenyltetrazolium chloride (TTC) (Cat# GP1047; Sevier Bio, China) and incubated at 37 °C for 15 min. After incubation, the brain tissue sections were removed and photographed. The percentage of infarction in all slices was calculated as the infarct area divided by the total brain tissue area.

TUNEL Detection of Apoptosis in Brain Tissues

The terminal deoxynucleotidyl transferase dUTP nick end labeling (TUNEL) assay, which uses a red fluorescence staining kit (Cat# G1502-50 T; Sevier Bio, China), was used to detect apoptotic cells in the tissue samples ($n = 6$). First, the tissue sections were heated at 64 °C for 1 h, dewaxed in xylene, and rehydrated through a series of alcohol gradients. The samples were then treated with proteinase K solution to increase the permeability of the staining agent, followed by washing with PBS (Cat# G0002-2 L, Sevier Bio, China). For labeling, each sample is incubated with TdT incubation buffer, which is a specific mixture of the recombinant TdT enzyme, biotin-dUTP labeling mixture, and balancing buffer. A negative control was prepared by replacing the TdT enzyme with ddH2O. After incubation, the samples were washed and then stained with DAPI (Cat# G1012-100ML; Sevier Bio, China) to visualize the nuclei and mounted with anti-fade mounting medium (Cat# G1401-5ML; Sevier Bio, China). The samples were examined under a fluorescence microscope, with apoptotic cells displaying red fluorescence and nonapoptotic cells displaying blue fluorescence.

Fluorescence In Situ Hybridization (FISH) and Immunofluorescence Dual Labeling

For FISH, miRNA-758-3p was labeled via the specific probe Fish-miR-758-3p (Abbott Laboratories, USA) with fluorescently labeled nucleotides for hybridization. Immunofluorescence staining was subsequently performed to detect the expression of integrin-linked kinase (ILK) ($n = 6$). Antigen retrieval was carried out with sodium citrate buffer (Cat# G0001-1L, Sevier Bio, China); endogenous peroxidase activity was quenched with blocking solution; nonspecific binding sites were blocked with 5% bovine serum albumin V; incubation was performed with a primary antibody against ILK (dilution 1:200, Cat# AF6141, Affinity Biosciences, Australia) and secondary antibody 488-labeled goat anti-rabbit IgG (dilution 1:200, Cat# GB25303, Sevier Bio, China); nuclei were stained with DAPI; slides were mounted with antifade mounting medium; the samples were observed and photographed under a fluorescence microscope. The fluorescence intensity was measured via Image-Pro Plus software to calculate the positivity rate.

Primary Cortical Neuron Isolation, Culture, and Oxygen–Glucose Deprivation Model Construction

To isolate and culture rat cerebral cortex neurons, the embryonic cerebral cortex was dissected, the meninges were removed, and the tissue was minced and digested with 0.25% trypsin (Cat# 9002–07-7; Meilunbio, China). The digestion was stopped with inoculation medium, the tissue was triturated and settled, and the supernatant was transferred and filtered. The cell suspension was centrifuged, and the pellet was resuspended to seed 1×107 cells in a 6-well plate. After 24 h, the medium was changed to DMEM/F12 (Cat# PWL038, Meilunbio, China) + 2% B27 (Cat# A1895601, Thermo Fisher Scientific, USA) for 3 days and then replaced with cytarabine to refine the culture. Neurons were cultured further, and the medium was replaced every 3 days. For the CIRI model, cells were exposed to hypoxic conditions in sugar-free medium for various durations and reoxygenated for up to 24 h, and a 2-h hypoxia and 24-h reoxygenation protocol was used for additional studies [33, 34].

Cell Counting Kit-8 (CCK-8) Assay for Cell Viability

To assess cell viability, we employed the CCK-8 method (Cat# CK04, Japan Torii Institute, Japan). Logarithmic growth phase cells from each group were seeded in a 96-well plate at a density of 5000 cells per well. After the cells were allowed to adhere, 10 µL of CCK-8 solution was added to each well, and the plate was incubated for 2.5 h. The optical density (OD) values were then read on a microplate reader.

Detection of Apoptosis by Flow Cytometry

To evaluate cell apoptosis, we utilized the ANNEXIN V-FITC/PI Apoptosis Detection Kit (Cat# CA1020, Solarbio, China) to assess apoptosis in various cell groups. The cells were centrifuged to collect (1 × 106 cells/mL) and washed with PBS to remove impurities from the culture medium. The cells were subsequently stained and stained with Annexin V and PI. The stained cells were then analyzed via flow cytometry.

Cell Transfection

In our study, to overexpress or knock down circRNA (0000964), miR-758-3p, and ILK, we utilized specialized lentiviral vectors provided by GeneCopoeia (USA). These vectors (0.5 μg of plasmid/well) were transfected into cultured neuronal cells via Lipofectamine 3000 (Cat# L3000015; Thermo Fisher Scientific, USA). The transfection process was conducted in strict accordance with the protocol provided by the manufacturer. Prior to transfection, the cells were cultured under standard conditions to ensure optimal growth. Posttransfection, the cells were further incubated under optimized conditions for 24 h, allowing the lentiviral vectors to efficiently introduce overexpression/silencing sequences into the neurons, resulting in the desired gene overexpression/silencing. All the experimental procedures were performed under aseptic conditions to ensure the accuracy and reproducibility of the results.

Immunofluorescence Detection of Neuronal Cells with TUJ1

Cell slides were prepared in advance to ensure normal cell status and proper adhesion. The cells were then incubated with primary antibody against TUJ1 (1:100, Cat# 26,048–1-AP, Proteintech, USA) and secondary antibody against goat anti-rabbit IgG labeled with 488 (dilution 1:200, Cat# GB25303, Sevier Bio, China). Nuclei were stained with DAPI (1 μg/mL), and slides were sealed with anti-fade mounting medium.

Dual-Luciferase Reporter Assay

The 3′UTR of ILK containing the miR-758-3p binding site was cloned and inserted into the psiCHECK-2™ (Promega, Madison, WI, USA) vector downstream of the luciferase gene. PC12 cells were transfected with the miR-758-3p mimic and the luciferase vector via Lipofectamine 3000. After 24 h, the Dual-Luciferase Reporter Assay System was used to measure luciferase activity. Renilla luciferase served as an internal control to normalize the transfection efficiency and expression levels. Luciferase activity data were analyzed to assess the impact of miR-758-3p on the ILK 3′UTR, and treated cells were compared with control cells.

circRNA Probe Affinity Enrichment Experiment

Total RNA was extracted from the lysate via a TRIzol Reagent Kit (Cat# 15596026; Thermo Fisher Scientific, USA) following the manufacturer's guidelines. The extracted RNA was mixed with biotinylated circRNA (0000964) probes (circRNA-F2, FITGENE) and incubated to form stable complexes. Streptavidin magnetic beads were added to bind the biotinylated probes, and the probe–RNA complexes were enriched via magnetic separation technology. The magnetic beads were washed multiple times with washing buffer to remove nonspecific binding or impurities. High salt buffer or heat treatment was used to dissociate the bound RNA from the beads, and the enriched RNA was collected. RT−PCR analysis was performed on the enriched RNA to determine the levels of miR-758-3p, and the interaction between the circRNA (0000964) and miR-758-3p was assessed.

RT−PCR

Total RNA from tissues or cells was extracted via the TRIzol Reagent Kit, followed by reverse transcription via the SureScript First-Strand cDNA Synthesis Kit (Cat# 11904018; Thermo Fisher Scientific, USA). The qPCRs were conducted using 2 × Universal Blue SYBR Green qPCR Master Mix (Cat# AB4163A; Thermo Fisher Scientific, USA). The qPCR protocol included a 1-min initial denaturation at 95 °C, followed by 40 cycles of denaturation at 95 °C for 20 s, annealing at 55 °C for 20 s, and extension at 72 °C for 30 s. The primers used are listed in the following table (Table 1). The calculation formula for mRNA expression is as follows: CmRNA = 2^-ΔΔCT, where ΔΔCT = ΔCT (experimental group)—ΔCT (control group), and ΔCT = CT (internal reference)—CT (target).

Western Blot

Proteins from tissues or cells were extracted via RIPA lysis buffer, and the protein concentration was determined via the BCA method (Cat# P0010; Beyotime, China). Proteins were denatured via 5 × sample buffer (Cat# G2075-1ML; Sevier Bio, China) and boiled for 10 min in a water bath. SDS−PAGE was used for protein separation, with preparatory stacking and resolving gels. Protein was transferred to PVDF membranes (Cat# WGPVDF22, Millipore, USA), after which nonspecific binding sites were blocked with 5% BSA (Cat# SW3015, Solarbio, China). The primary antibodies used were β-actin (dilution 1:25000, Cat# 66009–1-Ig, Proteintech, USA), ILK (dilution 1:1000, Cat# DF6141, Affinity, Australia), and Caspase3 (dilution 1:2000, Cat#

Table 1 Primers and sequences

Primers	Sequences
GAPDH-F	CCCATCACCATCTTCCAGG
GAPDH-R	CATCACGCCACAGTTTCCC
ILK-F	AATGGGACCCTGAACAAACAC
ILK-R	GCAAGCACCTAGTACCGGAAG
circ_0000495-F	CATCAGAAGCTGCCCTAACC
circ_0000495-R	TAACTCACCTGGGGGAAAAA
miR-758-3p F	GATGGTTGACCAGAGAGCACAC
miR-758-3p R	GTCGTATCCAGTGCAGGGT
U6-F	CTCGCTTCGGCAGCACA
U6-R	AACGCTTCACGAATTTGCGT
Caspase-3-F	AGGAGCAGTTTTGTGTGTGTG
Caspase-3-R	CTGAATGATGAAGAGTTTCGG

Ab184787, Abcam, USA). The secondary antibodies used were HRP-conjugated goat anti-rabbit IgG (dilution: 1:3000, Cat# GB23303; Servicebio, China) and HRP-conjugated goat anti-mouse IgG (dilution: 1:5000, Cat# GB23301; Servicebio, China). Visualization was achieved via the use of an enhanced chemiluminescence (ECL) substrate (KF8003, Affinity, China), followed by imaging and exposure. Densitometry was performed via ImageJ software, and the ratio of the target protein density to the internal reference density was calculated.

Data Analysis

To present and statistically analyze the experimental results in our study, we utilized GraphPad Prism 6.0 software (GraphPad Software, San Diego, CA). Initially, data collected from the experiments were input into Prism for graphical representation. Differences among multiple groups were assessed via analysis of variance (ANOVA). A p-value of < 0.05 was considered statistically significant. The data are presented as the means ± standard errors of the means (SEMs) or means ± standard deviations (SDs).

Results

Overexpression of miR-758-3p Promotes the Progression of CIRI

In this study, we investigated the role of miR-758-3p in a mouse CIRI model. We used an overexpression vector (OE-miR-758-3p) and confirmed its transfection efficiency via fluorescence microscopy (Fig. 1A). Despite stable body weights across groups, a slight decrease in the CIRI + OE-miR-758-3p group suggested a possible impact of miR-758-3p on energy metabolism (Fig. 1B). Behavioral scoring revealed worsened neurological deficits in the OE-miR-758-3p group (Fig. 1C), suggesting that miR-758-3p overexpression may exacerbate neurological damage. Additionally, CIRI volume was greater in the CIRI + OE-miR-758-3p group than in the other groups, which further highlights the potential of miR-758-3p in promoting CIRI (Fig. 1D).

Overexpression of miR-758-3p Promotes Apoptosis in Brain Tissue of CIRI Rats

TUNEL staining analysis revealed that the sham-operated control group had the lowest level of apoptosis. The CIRI model group displayed a significant increase in apoptosis. The CIRI + miR-758-3p + NC group had similar levels of apoptosis as the CIRI model group. Compared with the other groups, the CIRI + miR-758-3p group exhibited significantly greater levels of apoptosis (Fig. 2A, B). In summary, the overexpression of miR-758-3p significantly promoted apoptosis in the brain tissue of CIRI rats.

miR-758-3p and ILK Expression Levels Are Negatively Correlated

Through FISH dual labeling analysis, we explored the expression patterns and interrelationship of miR-758-3p and ILK in the CIRI model. We discovered colocalization of miR-758-3p and ILK in rat brain tissue. Compared with healthy brain tissue (sham group), in which ILK expression was at baseline, the nonspecific miRNA control (miR-758-3p-NC) did not significantly affect the changes in ILK expression induced by CIRI, further emphasizing the importance of specific miRNA regulation in the brain injury model. In the CIRI model treated with OE-miR-758-3p, significant downregulation of ILK expression was observed, which was negatively correlated with the overexpression of miR-758-3p, suggesting that miR-758-3p may exert its biological effects by downregulating ILK. On the other hand, miR-758-3p expression increased in the CIR model and further increased significantly in the model overexpressing miR-758-3p (Fig. 3A−C). These results indicate that miR-758-3p may affect the severity of CIRI injury by regulating ILK expression, suggesting a potential molecular mechanism.

Caspase-3, a member of the cysteine-aspartic protease family, plays a central role in the execution of cellular apoptosis. During CIRI, Caspase-3 is activated due to induced oxidative stress and inflammatory responses [35, 36]. Once it is activated, Caspase-3 initiates the apoptotic program by cleaving various intracellular substrates, such as poly ADP−ribose polymerase (PARP), resulting in the disruption of cellular structure and function and ultimately resulting in neuronal death [37, 38]. Therefore, Caspase-3 plays a decisive role in the neuronal damage and apoptosis caused by

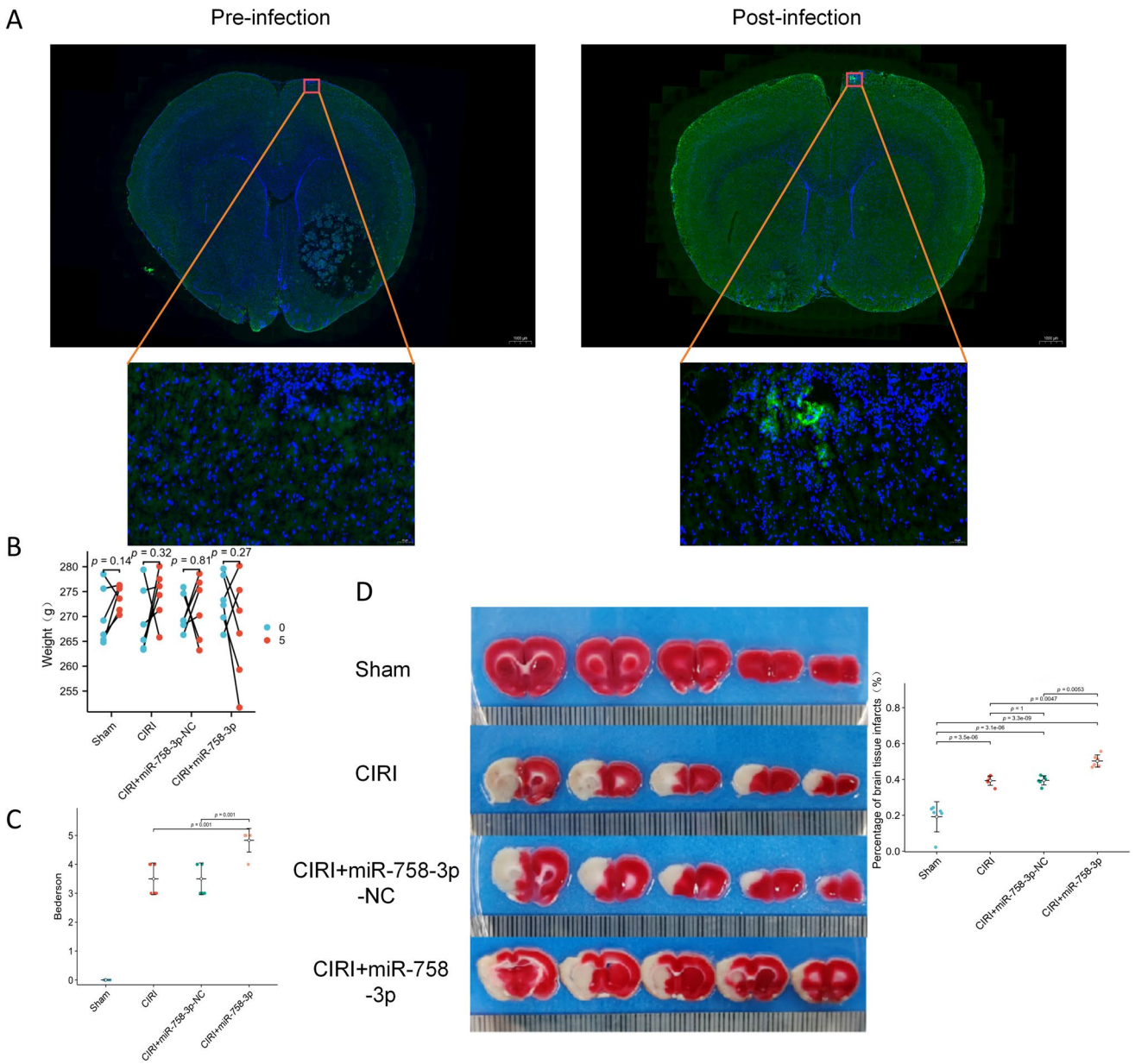

Fig. 1 Impact of miR-758-3p on the progression of CIRI in rats. **A** Fluorescence detection of OE-miR-758-3p lentivirus infection (the top image is the original image, while the bottom image is a 200×magnified version); **B** body weight records of each group of rats; **C** behavioral scores of each group of rats; **D** photographs of CIRI tissues from each group. $p > 0.05$ indicates that the difference between groups is not significant; $p < 0.05$ indicates that the difference between groups is significant

cerebral ischemia−reperfusion. In this study, we elucidated the regulatory effect of miR-758-3p on ILK expression and its inhibitory effect on Caspase-3 activation through RT−qPCR and western blot analyses. Compared with the sham group, the CIRI group presented significant increases in Caspase-3 and ILK expression. The introduction of a non-specific miR-758-3p negative control (miR-758-3p-NC) in the CIRI model did not affect the expression of these two proteins, thus emphasizing the necessity of specific miRNA regulation (Fig. 3D). When miR-758-3p was overexpressed in the CIRI model, ILK expression significantly decreased, whereas Caspase-3 expression significantly increased, confirming the strong regulatory effect of miR-758-3p on these two proteins (Fig. 3E, F).

In Vitro Simulation of CIRI Injury Model—Oxygen–Glucose Deprivation (OGD) Cell Model

In our study, TUJ1 staining was used to evaluate the effects of CIRI on rat cerebral cortical neurons in an

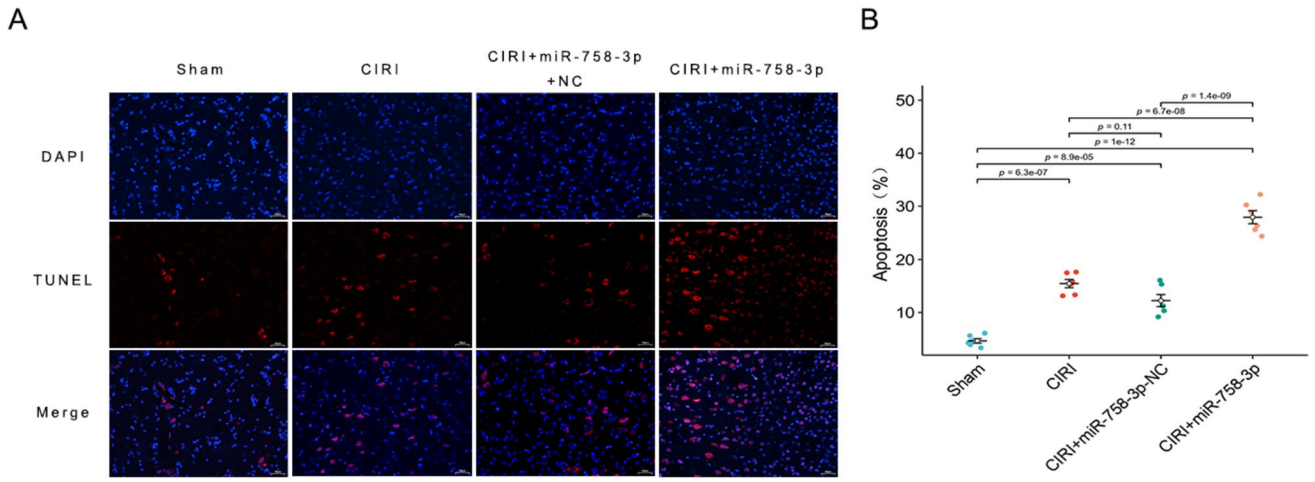

Fig. 2 miR-758-3p promotes apoptosis in CIRI tissue. **A** TUNEL assay for apoptosis in brain tissue (200×) and **B** percentage of apoptotic cells. $p > 0.05$ indicates that the difference between groups is not significant; $p < 0.05$ indicates that the difference between groups is significant

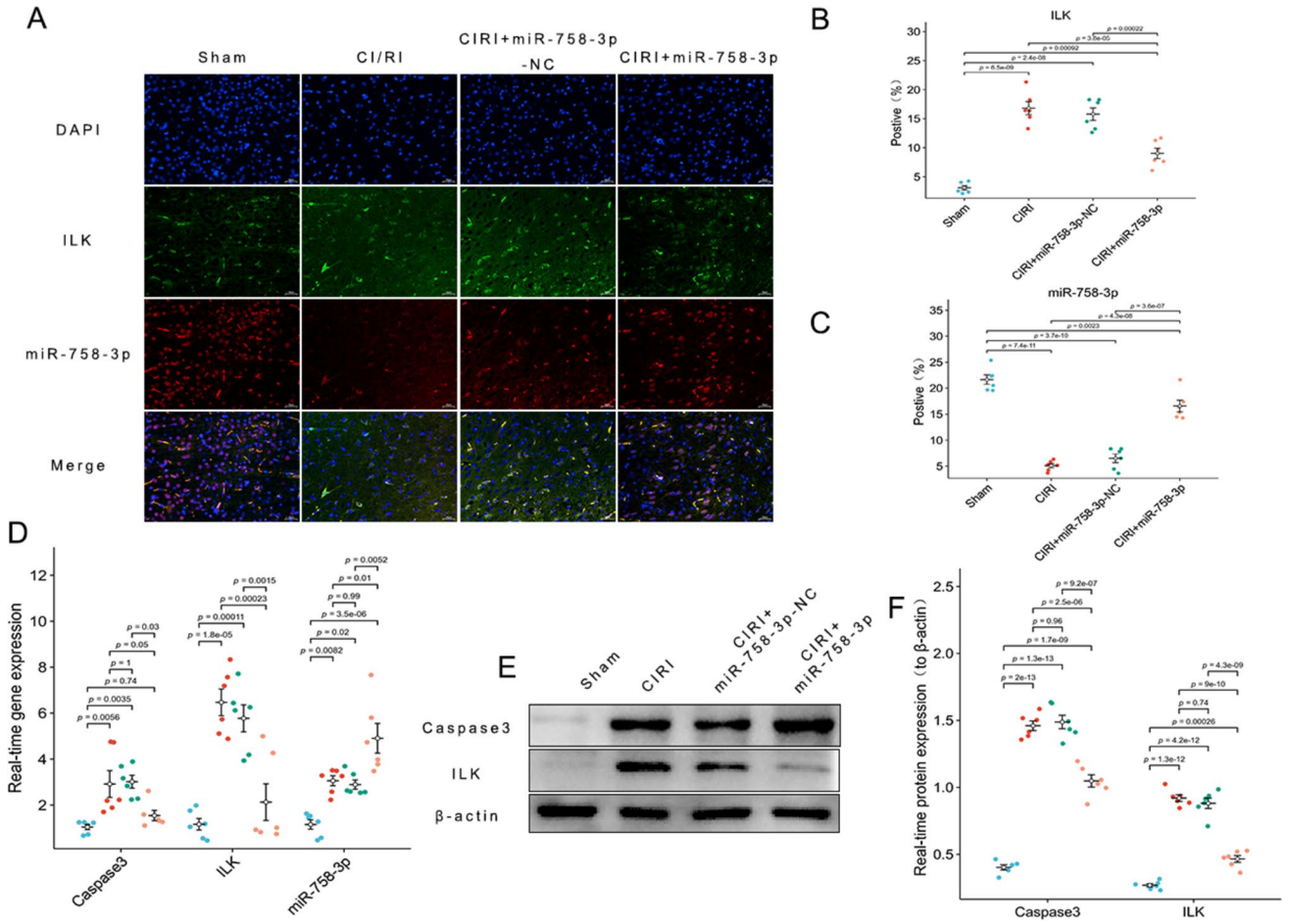

Fig. 3 Negative correlation between the miR-758-3p and ILK expression levels. **A** FISH double-staining for miR-758-3p and ILK expression (200X); **B, C** quantification of the fluorescence expression of ILK and miR-758-3p; **D** qRT−PCR analysis of Caspase-3, ILK, and miR-758-3p mRNA expression; **E** western blot analysis of Caspase-3 and ILK protein expression. $p > 0.05$ indicates that the difference between groups is not significant; $p < 0.05$ indicates that the difference between groups is significant

oxygen−glucose deprivation model (Fig. 4A). Neurons were exposed to hypoxia for 2, 4, or 6 h and then reoxygenated for 2 to 24 h. Notably, neurons subjected to 2 h of hypoxia followed by 24 h of reoxygenation presented a significant reduction in survival rate but maintained better growth than did those subjected to other conditions (Fig. 4B–E). This duration appeared optimal, balancing the effects of hypoxia without fully inhibiting neuronal growth. Our findings indicate that 24 h of reoxygenation posthypoxia effectively models CIRI, suggesting a critical timeframe to explore neuroprotective strategies.

ILK as a Target Gene of miR-758-3p

In this study, potential binding sites between ILK mRNA and miR-758-3p were initially identified through intersection analysis via the TargetScan, miRanda, and MicroCosm databases, with the aim of exploring the regulatory role of miR-758-3p in ILK (Fig. 5A). A dual-luciferase reporter assay confirmed a direct regulatory relationship between miR-758-3p and ILK (Fig. 5B). Further experimental results revealed that under OGD conditions, overexpression of miR-758-3p resulted in significant downregulation of ILK expression (Fig. 5C, D).

Overexpression of miR-758-3p Inhibits Neuronal Cell Activity, Which Is Mitigated by Overexpression of ILK

The overexpression of miR-758-3p reduced neuronal synapse quantity and morphology, and this effect was partially reversed by ILK, suggesting the role of ILK in mitigating the effects of miR-758-3p on neuronal activity (Fig. 6A−C). CCK-8 assays revealed reduced proliferation in neurons overexpressing miR-758-3p, which was increased by ILK overexpression, highlighting the importance of ILK in

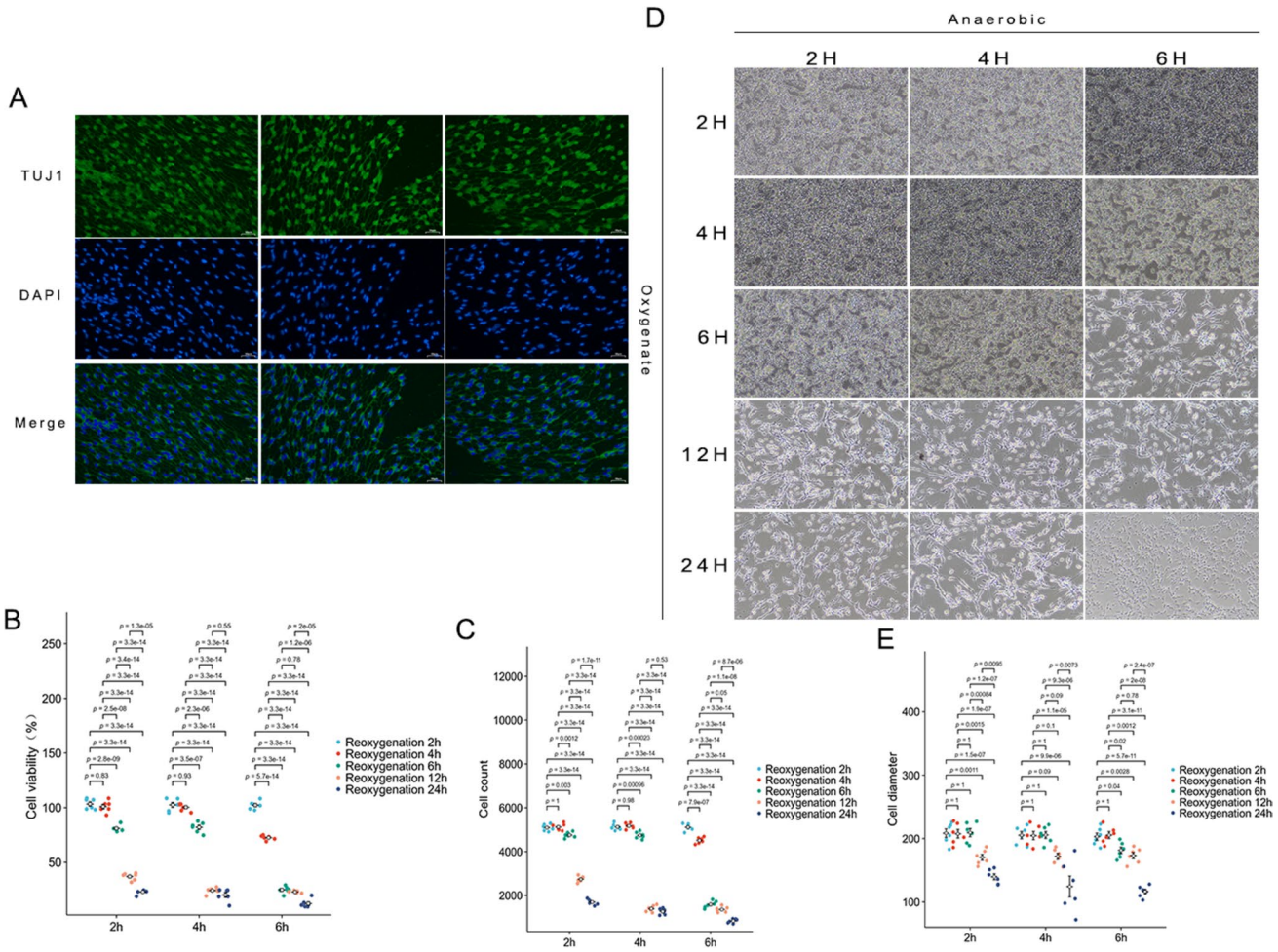

Fig. 4 Establishment of a CIRI injury model—the oxygen−glucose deprivation (OGD) model. **A** TUJ1 staining for neuron cell positivity (200×); **B** cell proliferation statistics for each group; **C** cell morphology observed under a microscope; **D** statistical analysis of the cell area in each group (100×); **E** cell count in each group. $p > 0.05$ indicates that the difference between groups is not significant; $p < 0.05$ indicates that the difference between groups is significant

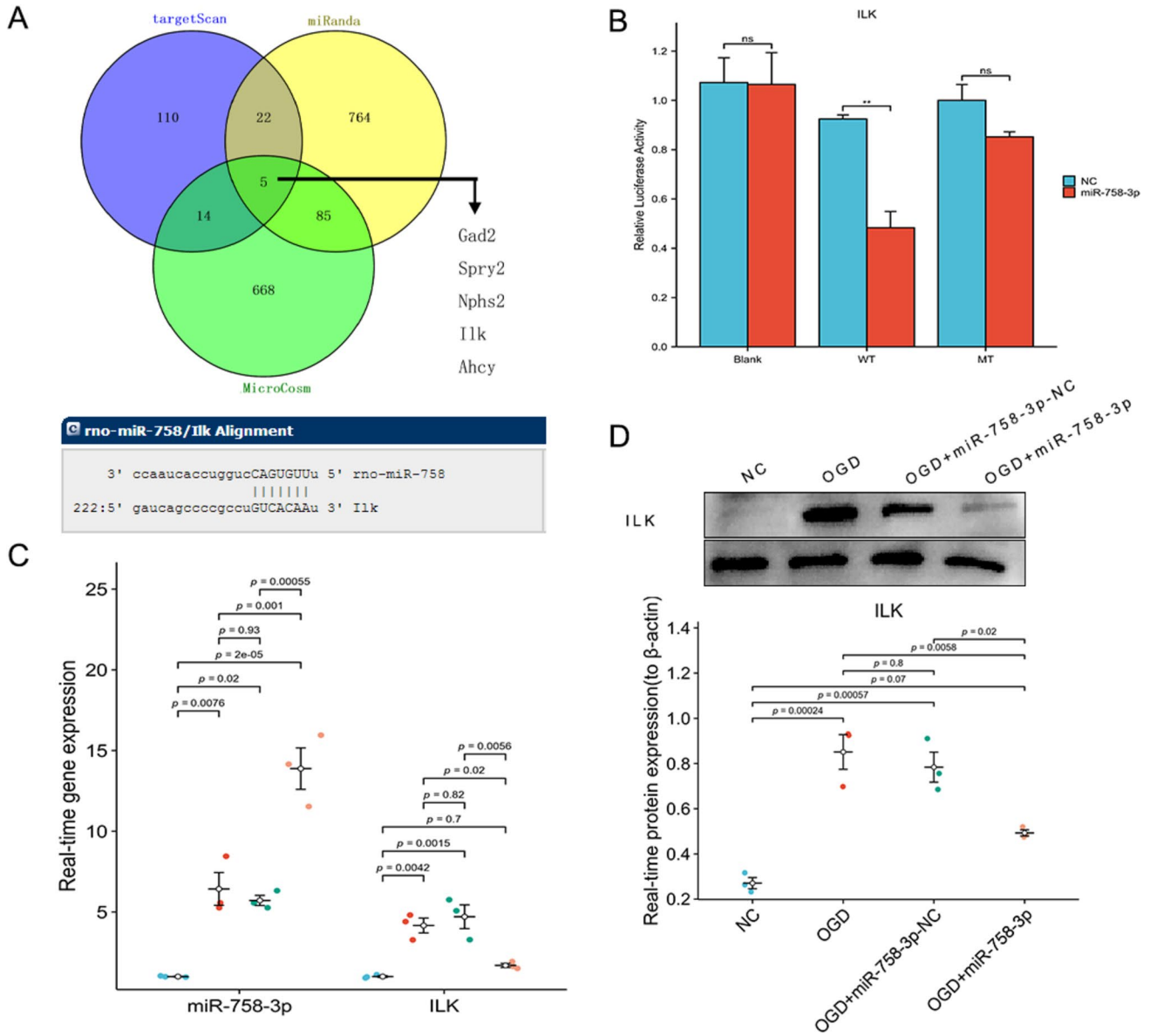

Fig. 5 Dual-luciferase assay identifying ILK as a target gene of miR-758-3p. **A** Predicted binding sites of ILK and miR-758-3p; **B** dual-luciferase assay validation of the relationship between miR-758-3p and ILK; **C** RT−PCR analysis of miR-758-3p and ILK mRNA expression; **D** western blot analysis of ILK protein expression. $p > 0.05$ indicates that the difference between groups is not significant; $p < 0.05$ indicates that the difference between groups is significant

neuronal survival and proliferation (Fig. 6D). TUJ1 expression decreased in neurons overexpressing miR-758-3p but was restored with ILK overexpression, demonstrating the protective role of ILK in maintaining neuronal integrity. The results of the western blot analysis revealed that the overexpression of miR-758-3p increased cleaved caspase-3 and caspase-3 levels and affected p-AKT and AKT expression, which was affected by ILK, particularly p-AKT, suggesting that ILK has the potential to promote neuronal survival signaling (Fig. 6E, F). These findings support the critical regulatory role of ILK in the context of miR-758-3p-induced neuronal inhibition, potentially through the AKT pathway, suggesting a target for therapeutic strategies to counter CIRI damage.

circRNA (0000964) Specifically Binds with miR-758-3p to Regulate ILK Expression

Next, we conducted transcriptome sequencing to identify differentially expressed circRNAs in the MCAO/R model group compared with the control group. The analysis revealed a total of 224 downregulated circRNAs.

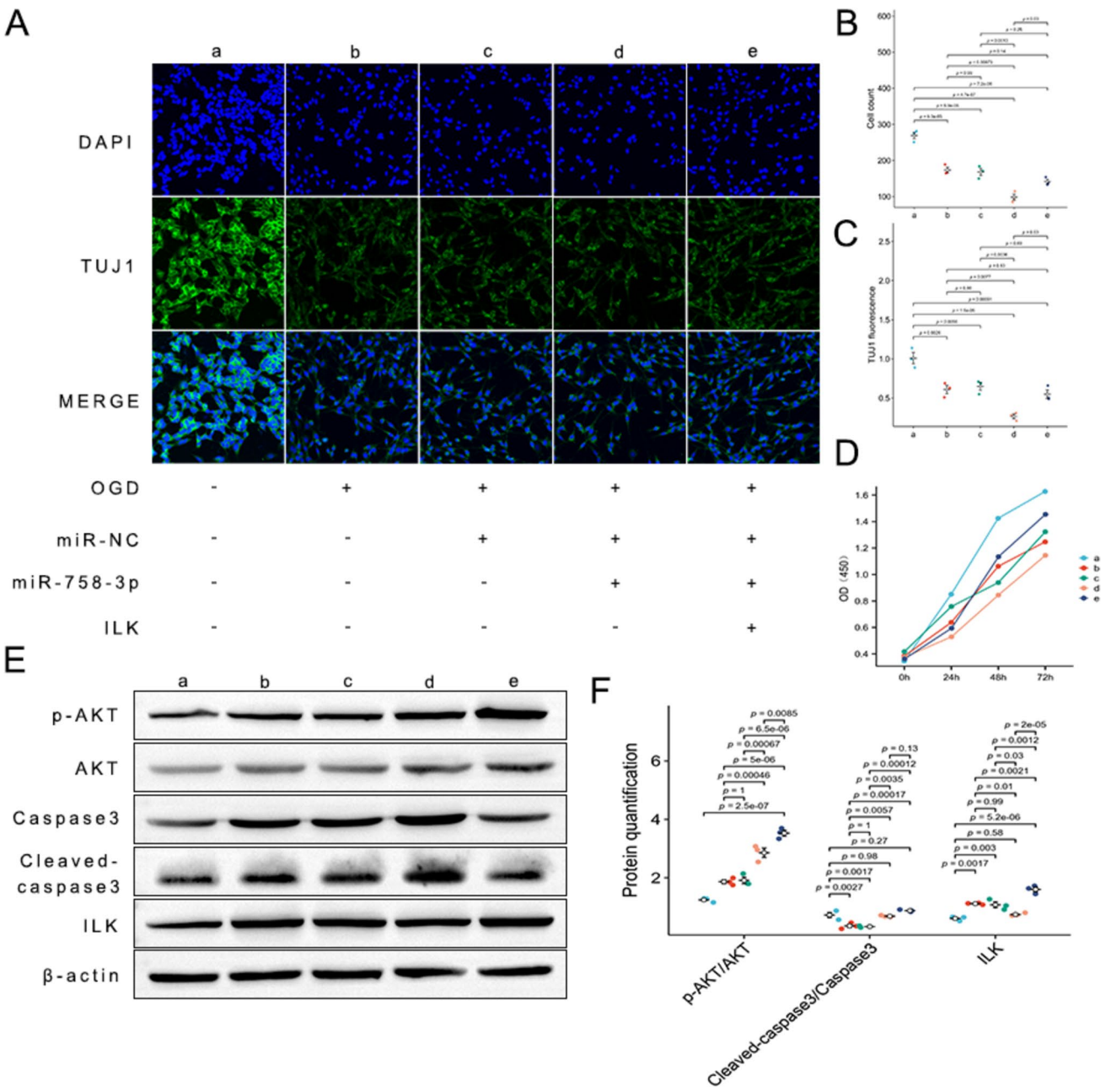

Fig. 6 miR-758-3p regulates neuronal activity via ILK. **A** Immunofluorescence detection of TUJ1 expression (200×); **B** cell count analysis; **C** statistical analysis of the cell area; **D** CCK-8 assay for cell proliferation activity; **F** western blot analysis of ILK, cleaved caspase-3, caspase-3, p-AKT, and AKT protein expression. $p > 0.05$ indicates that the difference between groups is not significant; $p < 0.05$ indicates that the difference between groups is significant

Bioinformatics predictions revealed 21 potential miR-758 targets. Through Venn diagram intersection analysis, we identified three potential circRNAs that may regulate miR-758: Novel_circ_0000964, Novel_circ_0002791, and Novel_circ_0004989. In our study, we selected Novel_circ_0000964 for subsequent experiments. We utilized lentivirus-mediated experiments to analyze the interactions between circRNAs (0000964), miR-758-3p, and ILK in rat cerebral cortical neurons. The groups included control, OGD, and variants with circRNA (0000964) and miR-758-3p silencing vectors. Affinity enrichment confirmed the specific binding of the circRNA (0000964) to miR-758-3p, indicating a targeting relationship (Fig. 7B). The levels of the enriched circRNA (0000964) and miR-758-3p increased, highlighting their direct interaction (Fig. 7C, D). Furthermore, mRNA analysis revealed that the expression

of a circRNA (0000964) was negatively correlated with the level of miR-758-3p, which inversely affected ILK expression (Fig. 7E). These findings demonstrate that circRNA (0000964) regulates ILK by sponging miR-758-3p, mitigating its inhibitory effect on ILK and hence supporting neuronal survival and influencing CIRI-induced neuronal repair mechanisms.

Overexpression of a circRNA (0000964) Mitigates the miR-758-3p-Induced Inhibition of Neuronal Cell Activity

Western blot analysis revealed that suppressing circRNA (0000964) significantly decreased ILK protein levels, whereas inhibiting miR-758-3p expression increased ILK levels (Fig. 8A). Synaptic density and structure were notably lower with circRNA (0000964) silencing than with miR-758-3p silencing, highlighting the role of circRNA (0000964) in mitigating the synaptic effects of miR-758-3p (Fig. 8B). Additionally, circRNA (0000964) silencing resulted in decreased neuronal cell viability and reduced TUJ1 expression, similar to the effects observed with miR-758-3p overexpression, suggesting that circRNA (0000964) counters the inhibitory effect of miR-758-3p on neuronal activity (Fig. 8C, D). Flow cytometry confirmed that reductions in ILK and TUJ1 are correlated with increased apoptosis (Fig. 8E, F). These findings highlight the pivotal role of the circRNA (0000964)/miR-758-3p/ILK axis in regulating neuronal viability.

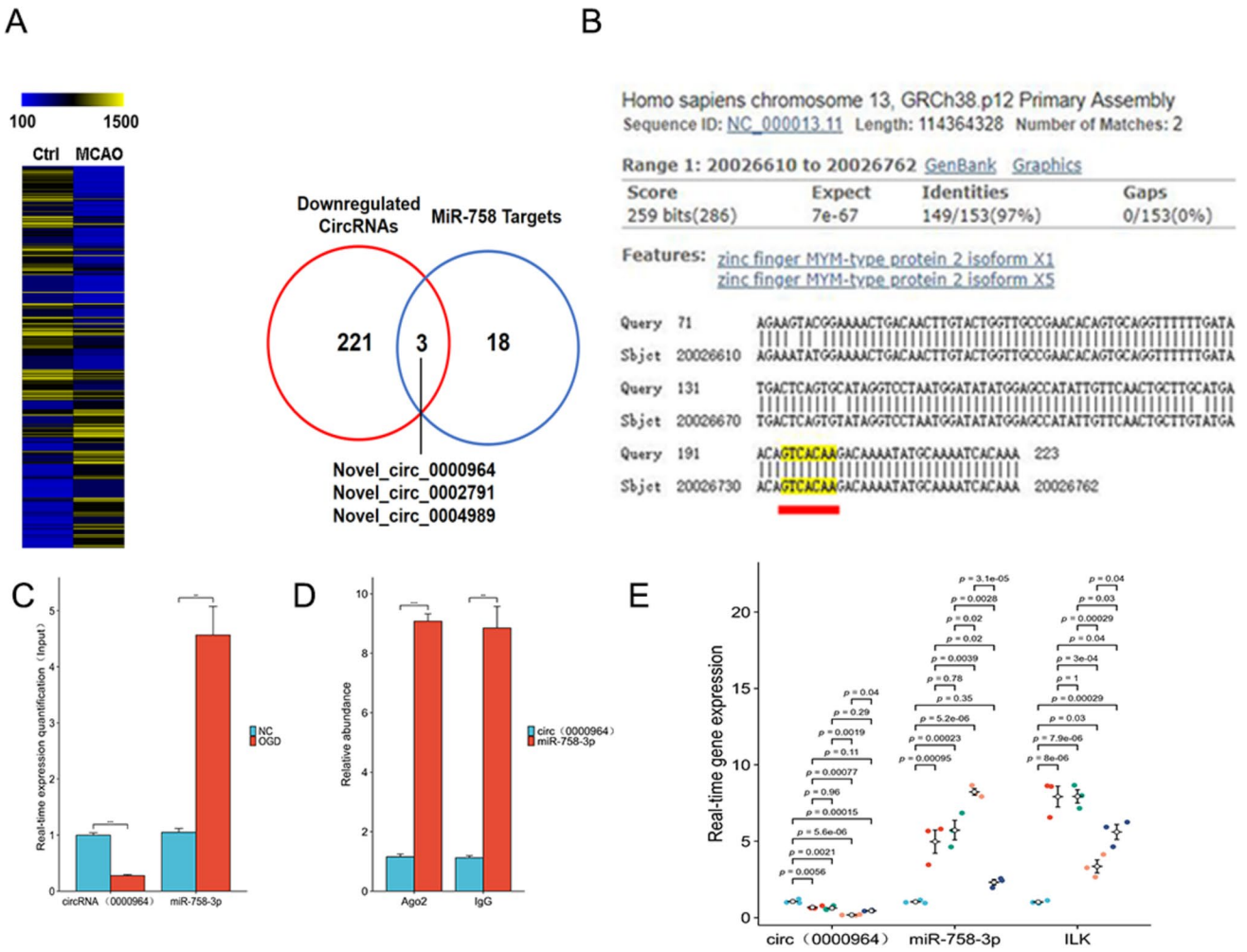

Fig. 7 Expression of ILK regulated by circRNA (0000964)/miR-758-3p. **A** Predicted binding of circRNA and miRNA; **B** potential binding sites between circRNA (0000964) and miR-758-3p; **C, D** enrichment of miR-758-3p by a circRNA (0000964) probe; **E** mRNA expression levels of circRNA (0000964)/miR-758-3p/ILK. $p > 0.05$ indicates that the difference between groups is not significant; $p < 0.05$ indicates that the difference between groups is significant

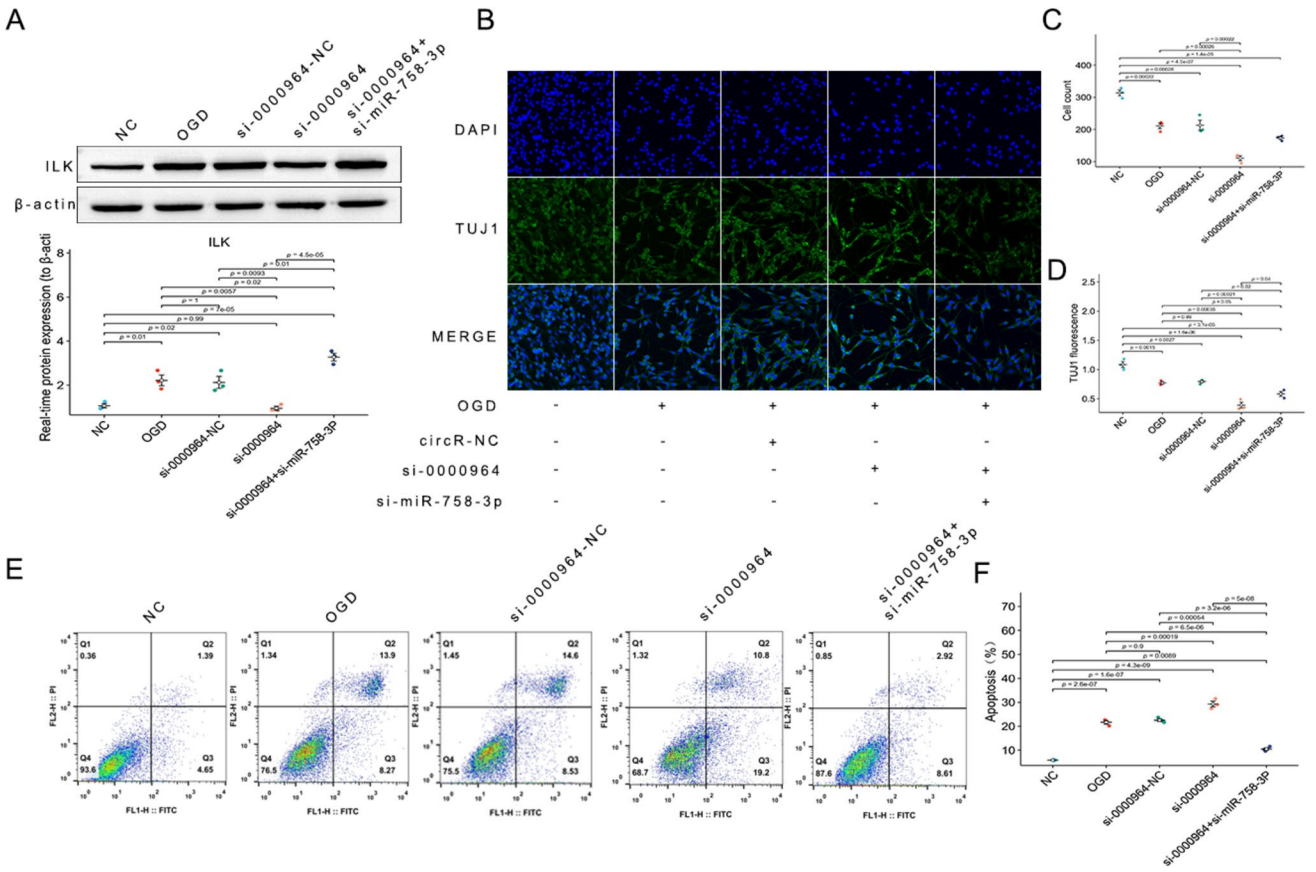

Fig. 8 Impact of circRNA (0000964)/miR-758-3p treatment on neuronal activity. **A** Western blot analysis of ILK protein expression; **B** confocal imaging of cells and TUJ1 fluorescence (200×); **C** quantification of neuronal cell count and **D** TUJ1 fluorescence intensity; **E** flow cytometry for detection of apoptosis and quantification (**F**). $p > 0.05$ indicates that the difference between groups is not significant; $p < 0.05$ indicates that the difference between groups is significant

Discussion

The core finding of this study is the elucidation of the critical roles of circRNA (0000964) and miR-758-3p in regulating ILK-mediated neuronal apoptosis, particularly under CIRI conditions. Extensive research has confirmed that circRNAs are widely involved in the regulation of neuronal cell damage [13]. For example, ciRS-7, a circRNA rich in miR-7 binding sites, is coexpressed in the mouse neocortex and in hippocampal neurons. ciRS-7 can bind to the RNA-induced silencing complex in a miR-7-dependent manner, upregulating the expression of miR-7 target genes and inhibiting the expression of α-synuclein, potentially offering neuronal protection [39, 40]. Additionally, circRNAs can participate in the protection or damage of neuronal cells by encoding peptides or proteins. For example, circHIPK3, derived from circularization of an exon of the HIPK3 gene and expressed in humans and mice, can encode the peptide HIPK3α, which has a protective effect on neurons [41]. In summary, circRNAs could become significant therapeutic targets for protection against ischemic stroke and other acute central nervous system injuries.

A key discovery in this study was the identification of integrin-linked kinase (ILK), a serine/threonine kinase widely expressed in various cells that plays a pivotal role in cell adhesion, migration, proliferation, differentiation, and survival [16, 42]. ILK is significantly involved in ischemia–reperfusion injury [43]. Research has highlighted the role of ILK in intracellular signal transduction, particularly upstream of the Akt and GSK-3beta pathways, by manipulating various cellular components [44]. Studies have also shown that ILK can protect neurons from damage by interfering with the activation of EGFP through the PI3K/Akt signaling pathway [45]. ILK expression increases in CIRI, promoting neuronal survival by activating the Akt pathway, and has been shown to protect cell survival via the NF-κB pathway in ovarian cancer studies [45, 46]. These findings increase our understanding of the critical role of ILK in the development of neuronal polarity.

We observed significant upregulation of ILK under CIRI conditions, which is consistent with the findings of previous

studies, indicating the crucial role of ILK in the neuronal response to ischemia−reperfusion stress. ILK activation may represent a self-protective mechanism aimed at increasing neuronal survival and reducing CIRI-induced damage. Thus, modulating ILK activity could be key to controlling CIRI injury. Recent research has revealed the importance of noncoding RNAs in neuroprotection and CIRI injury. For example, Yu et al. (2020) reported the protective role of specific miRNAs in ischemic brain injury, whereas Meng et al. (2020) explored how circRNAs regulate ischemic stroke by affecting neuronal apoptosis and neuroinflammation [47, 48]. We demonstrated that circRNA (0000964) expression decreases in the CIRI cell model, which is negatively correlated with the degree of neurological deficit. Studies have confirmed that miR-758-3p can regulate the vitality, apoptosis, and inflammation of human aortic endothelial cells through the BAMBI pathway in atherosclerosis and mediate cholesterol efflux through ABCA1 [27, 28]. Our research extends these findings, showing that a circRNA (0000964) and miR-758-3p can regulate ILK expression through a negative feedback loop, thus affecting neuronal apoptosis. We propose that the expression of a circRNA (0000964) decreases after CIRI and that the expression of miR-758-3p increases. This change in expression pattern may be a response to the cellular damage caused by CIRI. Importantly, we found that a circRNA (0000964) acts as a sponge for miR-758-3p, indirectly influencing ILK expression and activity by regulating the availability of miR-758-3p. This mechanism might constitute a cellular strategy to finely tune ILK activity and maintain cellular homeostasis.

Conclusion

The novelty and significance of our study lies in the discovery and validation of a regulatory network comprising a circRNA (0000964), miR-758-3p, and ILK, which collectively influence neuronal apoptosis in CIRI. This finding provides a new research perspective in the field, broadening the scope of noncoding RNAs in neuroprotection and offering potential targets for the development of novel therapeutic strategies [13, 49, 50].

Supplementary Information The online version contains supplementary material available at https://doi.org/10.1007/s12035-025-04736-5.

Author Contribution XL-M and XS-B wrote the manuscript of this study. Q-Z was involved in the study design and data collection. WW-Y, SX-L, L-X, and R-J analyzed and interpreted the data. XH-L, WJ-J, W-M, and M-Y assisted in the experimental procedures. FF-S and Y-Z directed the design and reviewed the manuscript. All authors reviewed the manuscript.

Funding The joint fund project of the Social Development Specialized Project of Yunnan Provincial Key Technology Research and Development Program, 202203AC100007 (to ZY). The National Natural Science Foundation of China, no. 81960219 (to XLM) and no. 82260246 (to XLM). Yunnan Province Applied Basic Research Joint Project, no. 202301AY070001-271 (to XLM).

Data Availability No datasets were generated or analysed during the current study.

Declarations

Ethics Approval All animal experimental procedures were carried out in accordance with relevant ethical guidelines and protocols and were approved by the Animal Experiment Ethics Committee of Kunming Medical University, approval number: kmmu20220412.

Conflict of Interest The authors declare no competing interests.

References

1. Feigin VL, Krishnamurthi RV, Parmar P, Norrving B, Mensah GA, Bennett DA, Barker-Collo S, Moran AE et al (2015) Update on the global burden of ischemic and hemorrhagic stroke in 1990–2013: the GBD 2013 study [J]. Neuroepidemiology 45(3):161–176
2. Liu L, Chen W, Zhou H, Duan W, Li S, Huo X, Xu W, Huang LA et al (2020) Chinese Stroke Association guidelines for clinical management of cerebrovascular disorders: executive summary and 2019 update of clinical management of ischaemic cerebrovascular diseases [J]. Stroke Vasc Neurol 5(2):159–176
3. Wang Y-J, Li Z-X, Gu H-Q, Zhai Y, Jiang Y, Zhao X-Q, Wang Y-L, Yang X et al (2020) China stroke statistics 2019: a report from the national center for healthcare quality management in neurological diseases, china national clinical research center for neurological diseases, the chinese stroke association, national center for chronic and non-communicable disease control and prevention, chinese center for disease control and prevention and institute for global neuroscience and stroke collaborations [J]. Stroke Vasc Neurol 5(3):211–239
4. Babu M, Singh N, Datta A (2022) In vitro oxygen glucose deprivation model of ischemic stroke: a proteomics-driven systems biological perspective [J]. Mol Neurobiol 59(4):2363–2377
5. Dong H, Wang S, Zhang Z, Yu A, Liu Z (2014) The effect of mitochondrial calcium uniporter opener spermine on diazoxide against focal cerebral ischemia–reperfusion injury in rats [J]. J Stroke Cerebrovasc Dis 23(2):303–309
6. Chen X, Li H, Huang M, Huang M, Xu W, Chu K, Chen L, Zhang Y (2014) Effect of Gua Lou Gui Zhi decoction on focal cerebral

ischemia-reperfusion injury through regulating the expression of excitatory amino acids and their receptors [J]. Mol Med Rep 10(1):248–254
7. Egashira Y, Suzuki Y, Azuma Y, Takagi T, Mishiro K, Sugitani S, Tsuruma K, Shimazawa M et al (2013) The growth factor progranulin attenuates neuronal injury induced by cerebral ischemia-reperfusion through the suppression of neutrophil recruitment [J]. J Neuroinflammation 10:105
8. Jurcau A, Simion A (2021) Neuroinflammation in cerebral ischemia and ischemia/reperfusion injuries: from pathophysiology to therapeutic strategies [J]. Int J Mol Sci 23(1):14
9. Imai F, Suzuki H, Oda J, Ninomiya T, Ono K, Sano H, Sawada M (2007) Neuroprotective effect of exogenous microglia in global brain ischemia [J]. J Cereb Blood Flow Metab 27(3):488–500
10. Guo Q, Kawahata I, Cheng A, Wang H, Jia W, Yoshino H, Fukunaga K (2023) Fatty acid-binding proteins 3 and 5 are involved in the initiation of mitochondrial damage in ischemic neurons [J]. Redox Biol 59:102547
11. Luo P, Fu X, Chang M, Zhang L, Guo L (2020) Cerebral ischemia-reperfusion causes a down regulation of HCN1 expression via enhancing the nuclear NRSF-HDAC4 gathering that contributes to neuron damage [J]. Brain Res Bull 156:50–57
12. Yuan L, Chen W, Xiang J, Deng Q, Hu Y, Li J (2022) Advances of circRNA-miRNA-mRNA regulatory network in cerebral ischemia/reperfusion injury [J]. Exp Cell Res 419(2):113302
13. Yang K, Zeng L, Ge A, Wang S, Zeng J, Yuan X, Mei Z, Wang G et al (2022) A systematic review of the research progress of non-coding RNA in neuroinflammation and immune regulation in cerebral infarction/ischemia-reperfusion injury [J]. Front Immunol 13:930171
14 Kapanova G, Tashenova G, Akhenbekova A, Tokpinar A, Yilmaz S (2022) Cerebral ischemia reperfusion injury: from public health perspectives to mechanisms [J]. Folia Neuropathol 60(4):384–389
15. Sharma D, Maslov LN, Singh N, Jaggi AS (2020) Remote ischemic preconditioning-induced neuroprotection in cerebral ischemia-reperfusion injury: preclinical evidence and mechanisms [J]. Eur J Pharmacol 883:173380
16 Górska A, Mazur AJ (2022) Integrin-linked kinase (ILK): the known vs. the unknown and perspectives [J]. Cell Mol Life Sci 79(2):100
17. Jiang S, Liang J, Li W, Wang L, Song M, Xu S, Liu G, Du Q et al (2023) The role of CXCL1/CXCR2 axis in neurological diseases [J]. Int Immunopharmacol 120:110330
18 Ulke-Lemée A, Macdonald JA (2010) Opportunities to target specific contractile abnormalities with smooth muscle protein kinase inhibitors [J]. Pharmaceuticals (Basel) 3(6):1739–1760
19 Bougea A, Angelopoulou E, Vasilopoulos E, Gourzis P, Papageorgiou S (2024) Emerging therapeutic potential of fluoxetine on cognitive decline in Alzheimer's disease: systematic review [J]. Int J Mol Sci 25(12):6542
20. Zhang Y, Zhu X, Huang C, Zhang X (2015) Molecular changes in the medial prefrontal cortex and nucleus accumbens are associated with blocking the behavioral sensitization to cocaine [J]. Sci Rep 5:16172
21. Li M, Dai F-R, Du X-P, Yang Q-D, Zhang X, Chen Y (2012) Infusion of BDNF into the nucleus accumbens of aged rats improves cognition and structural synaptic plasticity through PI3K-ILK-Akt signaling [J]. Behav Brain Res 231(1):146–153
22. Reventun P, Sánchez-Esteban S, Cook-Calvete A, Delgado-Marín M, Roza C, Jorquera-Ortega S, Hernandez I, Tesoro L et al (2023) Endothelial ILK induces cardioprotection by preventing coronary microvascular dysfunction and endothelial-to-mesenchymal transition [J]. Basic Res Cardiol 118(1):28
23. Urner S, Planas-Paz L, Hilger LS, Henning C, Branopolski A, Kelly-Goss M, Stanczuk L, Pitter B et al (2019) Identification of ILK as a critical regulator of VEGFR3 signalling and lymphatic vascular growth [J]. EMBO J 38(2):e99322
24. Zheng C-C, Hu H-F, Hong P, Zhang Q-H, Xu WW, He Q-Y, Li B (2019) Significance of integrin-linked kinase (ILK) in tumorigenesis and its potential implication as a biomarker and therapeutic target for human cancer [J]. Am J Cancer Res 9(1):186–197
25. Guerra BS, Lima J, Araujo B, Torres LB, Santos J, Machado D, Cunha E, Serrato JA et al (2021) Biogenesis of circular RNAs and their role in cellular and molecular phenotypes of neurological disorders [J]. Semin Cell Dev Biol 114:1–10
26 Neag M-A, Mitre A-O, Burlacu C-C, Inceu A-I, Mihu C, Melincovici C-S, Bichescu M, Buzoianu A-D (2022) miRNA involvement in cerebral ischemia-reperfusion injury [J]. Front Neurosci 16:901360
27. Wang Y, Chen X, Lu Z, Lai C (2022) Circ_0093887 regulated ox-LDL induced human aortic endothelial cells viability, apoptosis, and inflammation through modulating miR-758-3p/BAMBI axis in atherosclerosis [J]. Clin Hemorheol Microcirc 81(4):343–358
28. Li B-R, Xia L-Q, Liu J, Liao L-L, Zhang Y, Deng M, Zhong H-J, Feng T-T et al (2017) miR-758–5p regulates cholesterol uptake via targeting the CD36 3'UTR [J]. Biochem Biophys Res Commun 494(1–2):384–389
29. Shazeeb MS, King RM, Brooks OW, Puri AS, Henninger N, Boltze J, Gounis MJ (2020) Infarct evolution in a large animal model of middle cerebral artery occlusion [J]. Transl Stroke Res 11(3):468–480
30. Shanbhag NC, Henning RH, Schilling L (2016) Long-term survival in permanent middle cerebral artery occlusion: a model of malignant stroke in rats [J]. Sci Rep 6:28401
31. Bederson JB, Pitts LH, Tsuji M, Nishimura MC, Davis RL, Bartkowski H (1986) Rat middle cerebral artery occlusion: evaluation of the model and development of a neurologic examination [J]. Stroke 17(3):472–476
32 Xiao X-T, Luo C, Yuan Y, Xiao L, Qu W-S (2021) Systematic evaluation during early-phase ischemia predicts outcomes in middle cerebral artery occlusion mice [J]. Neuroreport 32(1):29–37
33. Hou K, Li G, Zhao J, Xu B, Zhang Y, Yu J, Xu K (2020) Bone mesenchymal stem cell-derived exosomal microRNA-29b-3p prevents hypoxic-ischemic injury in rat brain by activating the PTEN-mediated Akt signaling pathway [J]. J Neuroinflammation 17(1):46
34. Niu R-Z, Xiong L-L, Zhou H-L, Xue L-L, Xia Q-J, Ma Z, Jin Y et al (2021) Scutellarin ameliorates neonatal hypoxic-ischemic encephalopathy associated with GAP43-dependent signaling pathway [J]. Chin Med 16(1):105
35. Li Z, Xiao G, Wang H, He S, Zhu Y (2021) A preparation of Ginkgo biloba L. leaves extract inhibits the apoptosis of hippocampal neurons in post-stroke mice via regulating the expression of Bax/Bcl-2 and Caspase-3 [J]. J Ethnopharmacol 280:114481
36. Luan P, Xu J, Ding X, Cui Q, Jiang L, Xu Y, Zhu Y, Li R et al (2020) Neuroprotective effect of salvianolate on cerebral ischaemia-reperfusion injury in rats by inhibiting the Caspase-3 signal pathway [J]. Eur J Pharmacol 872:172944
37. Pan B, Sun J, Liu Z, Wang L, Huo H, Zhao Y, Tu P, Xiao W et al (2021) Longxuetongluo Capsule protects against cerebral ischemia/reperfusion injury through endoplasmic reticulum stress and MAPK-mediated mechanisms [J]. J Adv Res 33:215–225
38. Deng Z, Ou H, Ren F, Guan Y, Huan Y, Cai H, Sun B (2020) LncRNA SNHG14 promotes OGD/R-induced neuron injury by inducing excessive mitophagy via miR-182-5p/BINP3 axis in HT22 mouse hippocampal neuronal cells [J]. Biol Res 53(1):38
39. Shi Z, Chen T, Yao Q, Zheng L, Zhang Z, Wang J, Hu Z, Cui H et al (2017) The circular RNA ciRS-7 promotes APP and

BACE1 degradation in an NF-κB-dependent manner [J]. FEBS J 284(7):1096–1109
40. Hansen TB, Jensen TI, Clausen BH, Bramsen JB, Finsen B, Damgaard CK, Kjems J (2013) Natural RNA circles function as efficient microRNA sponges [J]. Nature 495(7441):384–388
41. Yin X, Zheng W, He L, Mu S, Shen Y, Wang J (2022) CircHIPK3 alleviates inflammatory response and neuronal apoptosis via regulating miR-382-5p/DUSP1 axis in spinal cord injury [J]. Transpl Immunol 73:101612
42. Dedhar S, Williams B, Hannigan G (1999) Integrin-linked kinase (ILK): a regulator of integrin and growth-factor signalling [J]. Trends Cell Biol 9(8):319–323
43. Margraf A, Germena G, Drexler HCA, Rossaint J, Ludwig N, Prystaj B, Mersmann S, Thomas K et al (2020) The integrin-linked kinase is required for chemokine-triggered high-affinity conformation of the neutrophil β2-integrin LFA-1 [J]. Blood 136(19):2200–2205
44. Guo W, Jiang H, Gray V, Dedhar S, Rao Y (2007) Role of the integrin-linked kinase (ILK) in determining neuronal polarity [J]. Dev Biol 306(2):457–468
45. Gary DS, Milhavet O, Camandola S, Mattson MP (2003) Essential role for integrin linked kinase in Akt-mediated integrin survival signaling in hippocampal neurons [J]. J Neurochem 84(4):878–890
46. Liu Q, Tan W, Che J, Yuan D, Zhang L, Sun Y, Yue X, Xiao L et al (2018) 12-HETE facilitates cell survival by activating the integrin-linked kinase/NF-κB pathway in ovarian cancer [J]. Cancer Manag Res 10:5825–5838
47. Qian Y, Chopp M, Chen J (2020) Emerging role of microRNAs in ischemic stroke with comorbidities [J]. Exp Neurol 331:113382
48. Lu M, Dong X, Zhang Z, Li W, Khoshnam SE (2020) Non-coding RNAs in ischemic stroke: roles in the neuroinflammation and cell death [J]. Neurotox Res 38(3):564–578
49. Mehta SL, Dempsey RJ, Vemuganti R (2020) Role of circular RNAs in brain development and CNS diseases [J]. Prog Neurobiol 186:101746
50. Gasparini S, Licursi V, Presutti C, Mannironi C (2020) The secret garden of neuronal circRNAs [J]. Cells 9(8):1815